Preprints of the 18th IFAC World Congress
Milano (Italy) August 28 - September 2, 2011

A Two Level Strategy for Combustion Engine Starter Robust Control in the Context of a Hybrid Power train

H. Luque[+#*], F. Claveau[#*], P. Chevrel[#*], F. Poil[+], F. Mercier-Calvairac[+]

**IRCCyN, Institut de Recherche en Communications et Cybernétique de Nantes, UMR CNRS 6597, 1 Rue de la Noë, B.P. 92101 - F-44321 Nantes, France*
(e-mail: fabien.claveau@mines-nantes.fr, philippe.chevrel@mines-nantes.fr)
[#]EMN, Ecole des Mines de Nantes, La Chantrerie, 4 Rue Alfred Kastler, B.P. 20722, 44307 Nantes Cedex 3, France
[+]PSA, Peugeot Citroën, 18 Rue des Fauvelles, 92250 La Garenne Colombes, France
(*e-mail: harry.luque@mpsa.com, frederic.poil@mpsa.com, fabien.merciercalvairac@mpsa.com*)

Abstract: The main difficulty in controlling combustion engine start-up comes from its changing behaviour from load to motor. In the context of hybrid power trains considered here, the electric motor used for start-up is more powerful than a traditional starter. In order to get a robust control of the crankshaft speed, we propose to take inspiration from redundant control as formulated in the aeronautic domain (Härkegard and Glad, 2005), (Buffington *et al.*, 1996), (Maciejowski, 1997), by considering that the engine and the electric motor are redundant torque providers. Despite that the engine is the primary torque provider, it will be systematically seen as the failing actuator during the start-up stage. Therefore, the electric motor has to compensate its deficiency.

Keywords: hybrid vehicles, engine start-up control, redundant actuators, daisy chaining, robust control.

1 INTRODUCTION

Traditionally, engine start-up is controlled using open loop control or some additional variable such as the intake air mass flow estimation as in (Ogawa and Ogai, 2008). In 2007, The SICE Research Committee on Advanced Power Train Control Theory provided a V6 gasoline engine model as a benchmark for advanced control methodologies (Ohata *et al.*, 2007). The model made of the engine and starter blocks combines continuous and discrete dynamic systems and includes a 46th order model with 13 inputs (throttle angle plus fuel injection and spark timing for each cylinder) and two outputs (engine speed and the air mass flow rate at the throttle). Based on this model, several control strategies were proposed in the literature: feedforward / feedback architecture involving particle swarm optimization and generalized predictive control, adaptative feedback linearization, etc, see *e.g.* (Zhang *et al.*, 2010), (Rokusho and Yamakita, 2008), (Sugihira and Ohmori, 2008), and references therein. However, this benchmark is specific to cold-start speed control of conventional internal combustion vehicles. It does not exactly suit the start-up speed engine problem of Hybrid Electric Vehicles (HEV) (Shui *et al.*, 2006).

Nowadays, the interest for the problem of engine start-up is renewed with the development of stop-start systems and full HEVs to reduce fuel consumption and emissions. For example, in a FUDS test driving cycle, the engine will be started about 65 times (Sugihira and Ohmori, 2008). This paper considers the problem of an engine start-up control system synthesis, which may be used to start the engine of a hybrid vehicle at rest or operating in an EV drive mode. Few papers exist on the subject, given that operating conditions are specific: the target idle speed can be higher than the conventional range of 600 to 800 rpm, the coolant temperature can be higher than the ambient temperature (*e.g.* 20°C), and more importantly, the starting motor is more powerful requiring new control strategies (Du *et al.*, 2008). At the beginning of the start-up stage, the electric motor has to produce the required torque, compensating for the combustion engine's resistance torque. Once the combustion engine has started running, during the second stage, the control architecture has to adapt the contribution of the electric motor according to the torque provided by the engine, in order to achieve the target speed in the best way, i.e. in a short time but without too much overshoot in engine speed. This second stage consists of multivariable control. The main difficulty of the control problem comes from the way the behaviour of the combustion engine changes between stages 1 and 2. Moreover, the engine model is very uncertain during start-up. To solve this control problem, we propose to take inspiration from control reconfiguration (Maciejowski, 1997, 1998), (Lunze and Richter, 2008) and also redundant control as formulated in the aeronautic domain, (Härkegard and Glad, 2005), (Buffington *et al.*, 1996), (Maciejowski, 1997).

The paper is organized as follows: in section 2, a specific control architecture for a scheme based on two redundant actuators is exhibited and analyzed, section 3 gives some rules to tune the controller before applying it to the hybrid vehicle engine start-up problem, in section 4, and finally, the whole control scheme is analyzed in terms of robustness and

performance before concluding.

2 CONTROL ARCHITECTURE

2.1 Presentation

In this subsection redundant control architecture is introduced in a general manner. Its (direct) adaptation to the control of the engine start-up of a hybrid power train is proposed in section 4. As discuss in subsection 2.3, this control architecture is based on the so-called "daisy-chaining" arrangement (Maciejowski, 1997, 1998), (Lunze and Richter, 2008). It is shown in Fig. 1, where A_1 and A_2 represent, respectively, primary and secondary actuators with unitary steady-state gains and L represents a generic load. A_1, A_2 and L make reference to both the physical systems and their respective models (potentially non-linear) depending on the context. The control architecture consists of a controller K and an estimator $(L^*)^{-1}$ which estimates the torque applied to the load L^*, which is an approximate model of the load L. The main signals are u, the global control input d, a disturbance r, the set point y, the outputs u_1 and u_2 delivered by actuators A_1 and A_2 respectively, and $\hat{v}_1$, the estimation of v.

The control architecture consists of two nested loops: an external loop (indicated in bold in Fig. 1) and an internal loop (within the external loop). The function of the internal loop is to guarantee a consistent behaviour of the system despite A_1 failure and the presence of d, while the external loop ensures set point tracking. The disturbance compensation can be distributed between the internal and external loops as a function of its frequency by tuning the estimator.

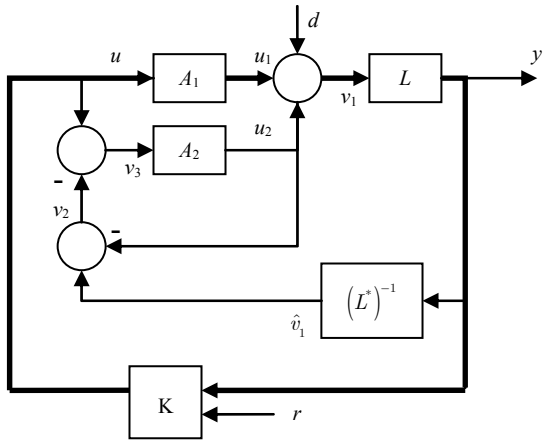

Fig. 1. Control architecture for redundant actuators scheme

2.2 General properties

The heart of the proposed control architecture is its internal loop which offers seamless reconfigurable control capabilities, as well as disturbance compensation in a desired bandwidth. The control architecture is able to provide these capabilities by dispatching one command signal among two actuators. A_1 receives the command signal directly, and in case of failure, A_2 will compensate for A_1 to obtain the desired behaviour. The behaviour of the system is guaranteed using the dynamics of A_2 to complement the primary actuator, A_1. That is, the over-actuated system behaves as if it had the auxiliary actuator only; however, it mainly uses the principal one. The following equations are used to calculate the "missing action", v_3, needed from the A_2 actuator to maintain the desired guaranteed output, y:

$$\begin{cases} v_1 = u_1 + u_2 + d \\ v_2 = v_1 \times L \times \left(L^*\right)^{-1} - u_2 \approx v_1 - v_2 = u_1 + d \\ v_3 = u - v_2 \approx u - \left(u_1 + d\right) \end{cases} \quad (1)$$

This 'missing action' accounts for the disturbance and the deficiency of A_1, which could be caused not only by actuator failure or saturation, but can also be caused by a slow response time or additional nonlinearities. Therefore, the internal loop can be used to assure a homogeneous behaviour in all situations using primarily A_1, using A_2 only when needed. The role of the external loop is to robustly reduce the controlled output's deviation from the reference r.

2.3 Comparison with other reconfigurable control strategies

Reconfigurable controls are designed to tolerate severe component faults such as failures (Blanke *et al.*, 2006). A survey on this research area can be found in: (Lunze and Richter, 2008) and (Zhang and Jiang, 2003, 2008). There are two types of reconfigurable control: active and passive. Active fault-tolerant control works by first detecting faults, then by changing the controller set point so as to match the desired output of the faulty plant. On the other hand, passive fault-tolerant control works with a fixed controller that provides a good behaviour despite the expected fault. In this paper we will focus on the passive fault-tolerant approach, looking for a robust controller which will function reliably in spite of a big disparity in the behaviour of the primary actuator, A_1. As stated in (Maciejowski, 1997, 1998), the simple daisy-chained arrangement and the constrained Model Based Predictive Control (MBPC) strategy are both able to solicit the back-up actuator if the command signal exceeds the saturation of the primary actuator. As the current behaviour of A_1 is assumed unknown, and for computation capacity reasons, the MBPC strategy is not considered further. The control architecture proposed in this paper is based on the daisy-chaining concept (Buffington and Enns, 1996), (Härkegard and Glad, 2005). As it will be shown later on, daisy-chaining does more than compensate for the failure of the A_1 actuator: it improves the primary actuator dynamics according to the capacity of A_2, leading to a (virtual) global actuator with the dynamics of A_2 and increased control amplitude. Finally, the proposed scheme dispatches the command between the two available actuators, guaranteeing a quasi-invariant behaviour in two situations: 1) the malfunction of the principal actuator (either by actuator failure or internal failure), and 2) the presence of disturbances.

2.4 Control architecture analysis

Let $w_2 = 1/\tau_2$ be the bandwidth of A_2 and assume the following hypotheses as true:
(H1): $L^* \approx L, \ \forall \omega << \omega_2$,

(H2): $\left|A_2\right|_{\omega<<\omega_2} = 1$,

(H3): $\left|A_1\right|_{\omega>\omega_2} << 0$.

Proposition 1: Consider Fig. 1. Under Hypotheses (H1) and (H2), the input-output relationship of the internal loop is:

$$\frac{y}{u} \approx LA_2, \quad \forall \omega << \omega_2, \text{ (for all } A_1\text{).} \tag{2}$$

Proof: Reducing the block diagram leads to:

$$\frac{y}{u} = L^* L\left(A_1 - A_1A_2 + A_2\right)\left(L^* + LA_2 - A_2L^*\right)^{-1}.$$

Applying (H1) leads to: $\frac{y}{u} \approx L\left(A_1\left(1-A_2\right)+A_2\right)$,

and finally, with (H2): $\frac{y}{u} \approx LA_2, \quad \forall \omega << \omega_2$ □

Proposition 2: Under (H1), the disturbance to output relationship of the internal loop is such that:

$$\frac{y}{d} \approx L - A_2, \quad \forall \omega << \omega_2 \tag{3}$$

Proof: this result comes from the direct application of (H1) to the transfer: $\frac{y}{d} = L^* L\left(1-A_2\right)\left(L^* + LA_2 - A_2L^*\right)^{-1}$. □

Remark: The internal loop compensates for a malfunction in the actuator A_1, and also cancels load input disturbances.

$$\frac{v_1}{d} = \left(1-A_2\right) \approx 0, \quad \forall \omega << \omega_2 \tag{4}$$

It is then clear that the schemes in figures 1 and 2 are equivalent in the bandwidth [0 ; ω_2]. This is the main property on which the external loop will be based on.

Remark: Assuming that hypothesis (H3) holds, meaning that the bandwidth of frequency actuator A_1 is less than that of actuator A_2, then the internal loop has the same behaviour as the system working with actuator A_2 only.

To conclude, the simplified scheme of Fig. 2 represents the equivalent behaviour of the global system.

$$\frac{e}{r} = \frac{1}{1+LA_2\mathrm{K}} \approx \frac{1}{1+L\mathrm{K}}, \qquad \frac{e}{d} = \frac{L\left(1-A_2\right)}{1+LA_2\mathrm{K}} \tag{5}$$

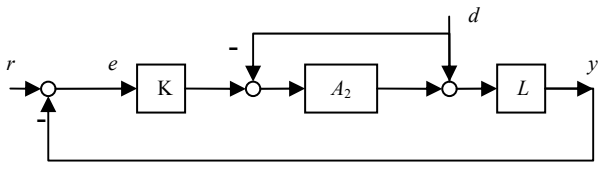

Fig. 2. External loop with simplified internal loop

3 TUNING METHODOLOGY

In the architecture shown in Fig. 1 and simplified in Fig. 2, each of the two loops has a clear function. The internal loop fixes a robust internal control (homogeneous input-output relationship between v_1 and u), and the external loop maintains the desired output, y. Given its imbricated nature, the internal loop must be tuned first to define the dynamics to which the external loop must react. The external loop control design is based on the system $L \times A_2$ as shown in §2.4.

The internal loop tuning exclusively consists of the dynamic estimation of v_1. This can be done thanks to a classical Luenberger observer, an unknown input observer (Darouach *et al.*, 1994), or simply by approximately inverting L as proposed in Fig. 1. The external loop has to perform robust control and tracking taking into account the residual uncertainties (and their location point) inside the internal loop.

4 APPLICATION

Because Hybrid Electric Vehicles (HEVs) are more expensive, they must offer additional benefits beyond their reduced environmental impact in order to be an attractive alternative to traditional internal combustion vehicles. Driveability is one aspect that has not been thoroughly studied and that could represent that extra advantage. One important component of driveability that is frequently encountered in HEV use is start-up of the combustion engine. In order to improve driveability, the start-up must occur quickly and seamlessly to react to traffic situations.

The ability of the previous control architecture to deal with the engine start-up of a hybrid vehicle will be evaluated. A Peugeot Citroën (PSA) parallel HEV prototype based on a diesel engine (120kW) and a synchronous motor (8kW) will be considered. The components involved during start-up are the engine, the DMF and the clutch, as seen in Fig. 3. The axle assembly consists of an engine (*ENG*) and an electric machine (*EM*), both considered with their local controllers, a double mass flywheel (*DMF*), and the clutch (*CLU*). The *DMF*, as its name indicates, can be roughly represented as two inertias (D_1 and D_2) connected by a spring-damper system (this model has been validated by comparison with a complete model of the DMF). As illustrated, one of the masses is linked to the engine and to the electric machine, while the other is connected to one of the clutch disks, (C_1).

Fig. 1 and Fig. 3 relate in the following way: the global control input u is the reference torque, v_3 is the reference torque for the *EM*, u_1 and u_2 the torque effectively generated by respectively *ENG* and *EM*, v_1 the global torque applied to D_1, and y the engine angular speed measure.

The control laws suggested by (Zhang *et al.*, 2010), (Rokusho and Yamakita, 2008), (Sugihira and Ohmori, 2008) for the SICE benchmark directly control throttle angle, the fuel injection, etc. to obtain the desired torque. In this paper, the proposed architecture generates the torque references for the engine and the electric motor, assuming that their local controllers determine the required throttle angle, current, etc..

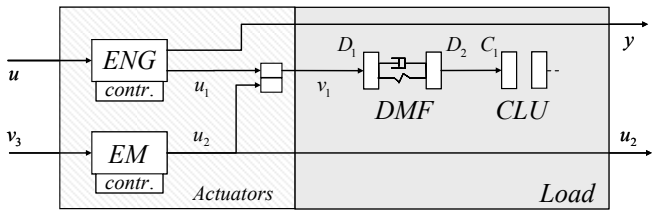

Fig. 3. Components

4.1 The start-up problem

The objective is to reach the desired angular speed at C_1 in the best possible way: quickly, seamlessly and with minimal overshoot. This can be achieved with the contributions of the engine and the electric machine. The principal actuator (referred as A_1 in §2) is the engine *ENG*, but it is not available at low rpms. Hence, the auxiliary actuator, A_2, which in this case is the electric machine, *EM*, is used in place of the ENG at low rpms. However, as soon as the engine is available, the demand on the electric machine, EM or A_2, is lowered while the demand on the engine is raised, allowing A_1 to become the primary source of actuation. When the engine is running, the engine and the electric machine are complementary in their torque output: the engine torque increases with rpms while the torque of the electric machine decreases.

More formally, the hybrid vehicle start-up problem has two control inputs, the engine and electric motor torque local references u and v_3, and two controlled outputs, the crankshaft speed (which should follow a given trajectory) and the electric motor torque, u_2 (which should be zero in steady state and should not compensate engine acyclisms at or above idling speed). The only measured outputs are the engine angular speed, y, and the electric motor torque, u_2.

4.2 Modelling

The simplified models supporting the control design will be presented in this section. They are indeed different from the much more complicated (and precise) models used for simulation of the engine-motor-flywheel system (see §5). As stated in (Kiencke and Nielsen, 2000) the engine (and its local controller) may be modelled after start-up by a first-order system with a delay where the time constant and delay depend on the engine speed. Before start-up, the model is very uncertain. Besides the resisting torque coming from compression, the most significant loss is friction loss, which mainly depends on the oil temperature (Bastard, 2006). Since the start-up occurs quickly, the temperature is considered to be constant throughout and the friction losses are represented as a constant disturbance, d. With the nomenclature used to present the architecture in Fig. 1, the simplified model after start-up is defined by:

$$Engine\left(A_1 : u \to u_1\right) : \frac{e^{-\tau_D s}}{\tau_{ENG} s + 1}, \text{ (after start-up)} \qquad (6)$$

where τ_{ENG} and $e^{-\tau_D s}$ are the time constant and delay of the engine, respectively, and are functions of the engine speed. Interval values are proposed in Table 1 considering an engine speed between 800 rpm and 3000 rpm.

The electric motor *EM* is modelled by:

$$Electric\ motor\left(A_2 : v_3 \to u_2\right) : \frac{1}{\tau_{EM} s + 1}, \qquad (7)$$

where τ_{EM} is the time constant of the EM. Finally, the load model, including the *ad hoc* inertias, damping and stiffness is:

$$Load\left(L : v_1 \to y\right) : \frac{I_2 s^2 + bs + k}{\left(I_1 I_2 s^2 + b\left(I_1 + I_2\right)s + k\left(I_1 + I_2\right)\right)s}, \qquad (8)$$

with I_1 representing the inertias of D_1, the *ENG* and *EM*, all of them with respect to the crankshaft. In turn, I_2 sums up the inertias of D_2 and C_1. The variables k and b denote the stiffness and the viscous damping coefficient of the spring-damper system in the DMF, respectively. Notice that if the dynamics of the DMF (oscillations around 13Hz) are neglected ($k \to +\infty$), the load model becomes:

$$L(s)_{k \to +\infty} \approx L_{rgd}(s) = \frac{1}{\left(I_1 + I_2\right)s} = \frac{1}{I_{CRA} s}, \qquad (9)$$

where $I_{CRA} = I_1 + I_2$ represents the total inertia at the crankshaft. The consequences of this simplification will be studied in the validation section.

4.3 The cascade controller

Tuning of the internal loop

Concerning the internal loop, as depicted in Fig. 1, the estimator is a filtered derivative. Its bandwidth was initially chosen to filter the engine acyclism frequencies corresponding to engine speeds above the idling speed. This choice was made to guarantee comfort during start-up by compensating for acyclic engine activity with the electric machine. At the same time, less energy is expended when not trying to compensate for acyclic activity at normal speeds. The estimator expression is the following:

$$\left(L^*\right)^{-1} = \frac{\left(L_{rgd}\right)^{-1}}{\alpha \tau_{ACY} s + 1} = \frac{\hat{v}_1}{y}, \text{ with } \frac{1}{\tau_{ACY}} = \frac{2 n_{IDL} C}{T} \cdot \frac{2\pi}{60} \qquad (10)$$

where n_{IDL} corresponds to the idling speed in rpm, C is the number of cylinders in the engine, T is the number of strokes required for one complete engine cycle, and α is a dimensionless factor to fine tune the filtering.

Tuning of the external loop

Although a simple PID could suffice for this particular application, the external loop controller, K, was designed using the Standard State Control (SSC) methodology. The SSC methodology (Chevrel, 2002), (Claveau *et al.*, 2008) leads to a H_2 optimization problem which is well-posed, and

easy to tune through high level design parameters to manage basic compromises between performances and robustness. Besides, it also facilitates a set point trajectory generation implementation. The model used to design the external loop controller is given by equation (5) and Fig. 2, with A_2 and L defined in equations (7) and (9).

5 CONTROL ANALYSIS AND VALIDATION

In this section, the properties of the internal loop are analyzed considering the hybrid start-up system. The model and control parameters used in simulation are given in Table 1.

Table 1. Parameter values

Parameter	Variable	Value
EM time constant	τ_{EM}	0.0167 s
D_1 inertia*	I_1	0.200 kg·m^2
D_2 inertia	I_2	0.084 kg·m^2
Total inertia at crankshaft	I_{CRA}	0.284 kg·m^2
DMF damping coefficient	b	1.6396 N·m/rad/s
DMF stiffness	k	433.5793 N·m/rad
Idling speed	n_{IDL}	800 rpm
ENG number of strokes	T	4
ENG number of cylinders	C	4
ENG time constant	τ_{ENG}	[20,75] ms
ENG delay	τ_D	[45,169] ms
Filter coefficient	α	2

*I_1 also includes the inertias of the engine and electric machine with respect to the crankshaft.

The filter coefficient α was chosen to filter the engine acyclisms above idling speed, n_{IDL}; the coefficient corresponds to a -6 dB gain at the idling speed acyclism frequency. With such tuning, the internal loop remains stable with a delay in the measurement of the engine angular speed, y, up to 20 ms, which is compatible with the control unit sampling period. Considering the whole control scheme proposed in Fig. 1, an infinite delay margin at the engine level confirmed the homogeneous input-output relationship between u and y demonstrated in §2.4.

To design the external loop controller K, the SSC methodology led to an observer – state feedback third-order control law. If such architecture is of interest in future experimental implementation, its transfer function is presented here to be concise:

$$\frac{u(s)}{y(s)} = \frac{-774.1(s+59.21)(s+9.337)}{s(s^2+140.6s+7066)}. \qquad (11)$$

Neglecting the exogenous signals d and r for robustness analysis, let us transform the whole system in Fig. 1 to the Linear Fractional Transformation (LFT) form of Fig. 4. Considering the H_∞ norm of M leads to:

$$\|M\|_\infty = 0.6066. \qquad (12)$$

Thanks to the small gain theorem (Zhou et. al, 1996), it is clear that the closed loop system will be stable if and only if:

$$\|A_1\|_\infty \le \frac{1}{0.6066} = 1.6485, \qquad (13)$$

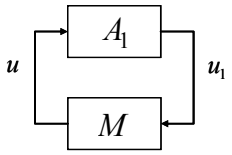

Fig. 4. Robustness analysis against engine model uncertainties

This confirms the robustness of the proposed architecture with regards to the engine. Furthermore, the architecture was tested using a sophisticated model (developed by the PSA's industrial research) that includes a zero-dimension thermodynamic engine model with mechanical and environmental losses and restrictions.

The upper graph shown in Fig. 5 evaluates the strategy's system performance by comparing the engine speed obtained using the proposed control strategy (signals "ENG" and "D2", respectively the engine and D2 angular speeds) to the speed obtained by demanding the maximum (saturation) engine and electric motor torques (signals "ENG_sat" and "D2_sat"). As can be observed, the strategy does not slow down the system significantly, but it slightly reduces oscillations around 200 ms and attains the 3000 rpm set point smoothly. The lower graph of Fig. 5 shows engine and electric machine torques, using the proposed architecture, highlighting how the engine and electric machine complement each other. When the engine speed is low, the engine is not capable of producing torque. In fact, it consumes torque. Later, around 200 ms, as the engine begins to be effective, the torque provided by the electric machine is reduced. The results obtained also show the inherent capability of the architecture to always direct the highest demand to the principal actuator, while relying on the second only in cases where the primary actuator is not sufficient.

The results obtained with a 1000 rpm set point are presented in Fig. 6. It is important to highlight the good compromise between smoothly attaining the desired engine speed, damping the oscillation and the reactivity (system stabilisation occurs at around 350 ms). This result is even more remarkable, taking into account the low set point, since at low rpms the acyclic activity in the engine is stronger and the system is closer to the DMF's natural frequency.

6 CONCLUSIONS

Hybrid vehicle start-up is often solved by automakers by using open loop control strategies, which have to be carefully conceived and fine tuned for each particular group of components, hindering the control method portability. These traditional control schemes also imply the definition of thresholds, to anticipate the engine's start-up of the engine. However, since not all start-ups are the same, the thresholds have to be set to the worst known case scenario. Finally, even if the target is an angular speed, this approach requires a

specific control strategy for start-up and another strategy for angular speed regulation. This raises the question of when to switch from one strategy to the other. The proposed control architecture overcomes this drawback, while being simple. Moreover, it is sufficiently general to be extended to more complex applications (e.g. speed vehicle control during transient states). Finally, the architecture combined with an *ad hoc* unknown input observer is a promising way to deal with a large class of fault-tolerant control problems.

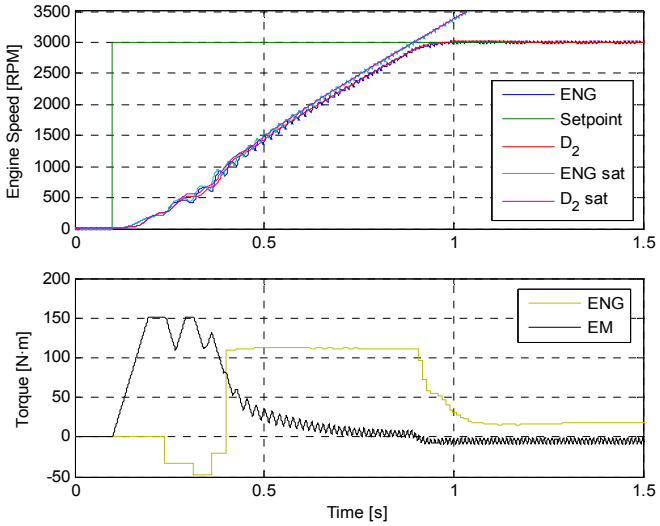

Fig. 5. Simulation results for a 3000 rpm set point

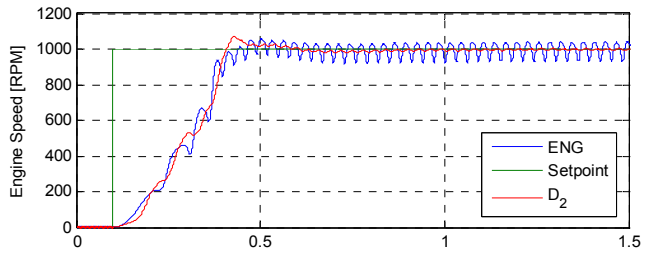

Fig. 6 Simulation results for a 1000 rpm set point

7 REFERENCES

Bastard, P. and Vallet, F. (2006). Simulation du démarrage à froid des véhicules automobiles. In *Proceedings of the LMCS'2006* (in French).

Blanke M., Kinnaert M., Lunze J., and Staroswiecki J. (2006). Diagnosis and Fault-Tolerant Control. *Springer, 2nd edition*.

Buffington, J. M. and Enns, D. F. (1996). Lyapunov stability analysis of daisy chain control allocation. *Journal of Guidance, Control, and Dynamics*, 19(6):1226-1230, Nov.-Dec. 1996.

Chevrel, Ph. (2002). Commande des systèmes Linéaires. In Ph. de Larminat, *Méthodologie de la commande par l'approche d'état*, 151-192, Hermès, Paris. (in french)

Claveau, F., Chevrel, Ph., Knittel, D. (2008). A two degrees of freedom gain-scheduled controller design methodology for a multi-motors web transport system. *IFAC Control Engineering Practice, 16*(5):*609-622*.

Darouach, M., Zasadzinski, M., and Xu, S.J. (1994). Full-order observers for linear systems with unknown inputs. *IEEE Transaction on Automatic Control*, 39:606–609.

Du, A., Lou, G. , Zhuang, J. , Xu, G. , and Xu, K. (2008). Hybrid electric vehicle quick start capability using integrated starter-generator. In *Proceedings of the IEEE Vehicle Power and Propulsion Conference*, Harbin, China.

Härkegard, O. and Glad, S.T. (2005). Resolving actuator redundancy—optimal control vs. control allocation. *Automatica,* 41:137 – 144.

Kiencke, U. and Nielsen, L. (2000). *Automotive Control Systems For Engine, Driveline, and Vehicle*. Springer-Verlag, Berlin.

Lunze, J. and Richter, J.H. (2008). Reconfigurable fault-tolerant control: a tutorial introduction. *European Journal of Control*, 14(5): 359-390.

Maciejowski, J.M. (1997). Reconfigurable control using constrained optimization. In *Proceedings of the European Control Conference*, Semi-plenary paper, Brussel, Belgium.

Maciejowski, J.M. (1998). The implicit daisy-chaining property of constrained predictive control. *Applied Maths and Computing Science*, 8(4):695-711.

Ohata, A., Kako, J., Shen, T. and Ito, T. (2007). Benchmark problem for automotive engine control. In *Proceedings of the 2007 Annual Conference SICE*, Takamatsu, Japan.

Ogawa, M. and Ogai, H. (2008). The cold starting control of engine using Large scale database-based Online Modelling. In *Proceedings of the 17th IFAC World Congress*, Seoul, Korea.

Rokusho, T. and Yamakita, M. (2008). Robust Combined feedforward and feedback control for start-up engine control. In *Proceedings of the IEEE International Conference on Systems and Control*, San Antonio, USA.

Shui, Y., Liguang, L., Guangyu, D., Xusheng, Z. (2006). A Study of Control Strategies of PFI Engine during Cranking and Start for HEVs. In *Proceedings of the IEEE International Conference on Vehicular Electronics and Safety*, Beijing, China.

Sugihira, S. and Ohmori, H. (2008). Model based starting control of SI engines via adaptive feedback linearization. In *Proceedings of the* 2008 *Annual Conference SICE*, Tokyo, Japan.

Zhang, Y. and Jiang, J. (2003). Bibliographical review on reconfigurable fault-tolerant control systems. In *Proceedings of the 5th IFAC Symposium on Fault Detection, Supervision and Safety for Technical Processes*, Washington D.C., USA.

Zhang, Y. and Jiang, J. (2008). Bibliographical review on reconfigurable fault-tolerant control systems. *Annual Reviews in Control*, 32:229-252.

Zhang, J., Shen, T. and Marino, R. (2010). Model-based cold-start speed control scheme for spark ignition engines. *Control Engineering Practice*, 2010 doi:10.1016/j.conengprac.2010.01.010

Zhou C., Doyle J.C., Glover K., (1996). Robust and optimal control. *Prentice Hall,* USA.